



## HESS J1023–575: Non-thermal particle acceleration associated with the young stellar cluster Westerlund 2

O. REIMER<sup>1</sup>, J. HINTON<sup>2</sup>, W. HOFMANN<sup>3</sup>, S. HOPPE<sup>3</sup>, C. MASTERSON<sup>4</sup>, M. RAUE<sup>5</sup>,  
FOR THE H.E.S.S. COLLABORATION<sup>6</sup>.

<sup>1</sup> *Stanford University, HEPL & KIPAC, Stanford, CA 94305-4085, USA*

<sup>2</sup> *School of Physics & Astronomy, University of Leeds, Leeds LS2 9JT, UK*

<sup>3</sup> *Max-Planck-Institut für Kernphysik, P.O. Box 103980, 69029 Heidelberg, Germany*

<sup>4</sup> *Dublin Institute for Advanced Studies, 5 Merrion Square, Dublin 2, Ireland*

<sup>5</sup> *Universität Hamburg, Institut für Experimentalphysik, Luruper Chaussee 149, 22761 Hamburg, Germany*

<sup>6</sup> [http://www.mpi-hd.mpg.de/hfm/HESS/public/hn\\_hesscollab.html](http://www.mpi-hd.mpg.de/hfm/HESS/public/hn_hesscollab.html)

*olr@stanford.edu; martin.raue@desy.de*

**Abstract:** The results from H.E.S.S. observations towards Westerlund 2 are presented. The detection of very-high-energy gamma-ray emission towards the young stellar cluster Westerlund 2 in the HII complex RCW49 by H.E.S.S. provides ample evidence that particle acceleration to extreme energies is associated with this region. A variety of possible emission scenarios is mentioned, ranging from high-energy gamma-ray production in the colliding wind zone of the massive Wolf-Rayet binary WR 20a, collective wind scenarios, diffusive shock acceleration at the boundaries of wind-blown bubbles in the stellar cluster, and outbreak phenomena from hot stellar winds into the interstellar medium. These scenarios are briefly compared to the characteristics of the associated new VHE gamma-ray source HESS J1023–575, and conclusions on the validity of the respective emission scenarios for high-energy gamma-ray production in the Westerlund 2 system are drawn.

## The young stellar cluster Westerlund 2 in the HII region RCW 49

The prominent giant HII region RCW 49, and its ionizing young stellar cluster Westerlund 2, are located towards the outer edge of the Carina arm of our Milky Way. RCW 49 is a luminous, massive star formation region, and has been extensively studied at various wavelengths. Recent mid-infrared measurements with SPITZER revealed still ongoing massive star formation [1]. The regions surrounding Westerlund 2 appear evacuated by stellar winds and radiation, and dust is distributed in fine filaments, knots, pillars, bubbles, and bow shocks throughout the rest of the HII complex [2, 3]. Radio continuum observations revealed two wind-blown shells in the core of RCW 49 [4], surrounding the central region of Westerlund 2, and the prominent Wolf-Rayet star WR 20b. A long-standing distance ambiguity has

been recently [5] revised in a determination of the distance to Westerlund 2 by spectro-photometric measurements of 12 cluster member O-type stars of  $(8.3 \pm 1.6)$  kpc. This value is in good agreement with the measurements from the light curve of the eclipsing binary WR 20a [6], associating WR 20a as a cluster member of Westerlund 2 (Note, however the 2.8 kpc as of [20]). The stellar cluster contains an extraordinary ensemble of hot and massive stars, presumably at least a dozen early-type O-stars, and two remarkable WR stars. Only recently WR20a was established to be a binary [7, 8] by presenting a solutions for a circular orbit with a period of 3.675, and 3.686 days, respectively. Based on the orbital period, the minimum masses have been found to be  $(83 \pm 5) M_{\odot}$  and  $(82 \pm 5) M_{\odot}$  for the binary components [6]. At that time, it classified the WR binary WR 20a as the most massive of all confidently measured binary systems in our Galaxy. The supersonic stellar winds of both WR stars collide, and a wind-wind interaction zone forms at the

stagnation point with a reverse and forward shock. In a detached binary system like WR 20a, the colliding wind zone lies between the two stars, and is heavily skewed by Coriolis forces. The winds of WR 20a can only be accelerated to a fraction of their expected wind speed  $v_\infty \sim 2800$  km/s, and a comparatively low pre-shock wind velocity of  $\sim 500$  km/s follows. Synchrotron emission has not yet been detected from the WR 20a system, presumably because of free-free-absorption in the optically thick stellar winds along the line of sight. WR 20a has been detected in X-rays [9], but non-thermal and thermal components of the X-ray emission remain currently indistinguishable. Detectable VHE gamma-radiation from the WR 20a binary system was only predicted in a pair cascade model [10], although detailed modeling of the WR 20a system in other scenarios (e.g. as of [11] when produced either by optically-thin inverse Compton scattering of relativistic electrons with the dense photospheric stellar radiation fields in the wind-wind collision zone or in neutral pion decays, with the mesons produced by inelastic interactions of relativistic nucleons with the wind material) is still pending. At VHE gamma-rays, photon-photon absorption will diminish the observable flux from a close binary system such as WR 20a [12].

## H.E.S.S. observations of Westerlund 2

The H.E.S.S. (High Energy Stereoscopic System) collaboration observed the Westerlund 2 region between March and July 2006, and obtained 14 h (12.9 h live time) of data, either on the nominal source location of WR 20a or overlapping data from the ongoing Galactic plane survey. Standard quality selections were imposed on the data. The data have been obtained in wobble-mode observations to allow for simultaneous background estimation. The wobble offsets for these observations range from  $0.5^\circ$  to  $2^\circ$ , with the majority of data taken with wobble offset less than  $0.8^\circ$ . The zenith angles range between  $36^\circ$  and  $53^\circ$ , resulting in an energy threshold of 380 GeV for the analysis. The data have been analyzed using the H.E.S.S. standard Hillas analysis with standard cuts ( $> 80$  p.e.). A point source analysis on the nominal position of WR 20a resulted in a clear signal with a significance of  $6.8\sigma$ . Further investigations revealed

an extended excess with a peak significance exceeding  $9\sigma$  (Fig.3 left). The center of the excess was derived by fitting the two-dimensional point spread function (PSF) of the instrument folded with a Gaussian to the uncorrelated excess map:  $\alpha_{2000} = 10^h 23^m 18^s \pm 12^s$ ,  $\delta_{2000} = -57^\circ 45' 50'' \pm 1' 30''$ . The systematic error in the source location is  $20''$  in both coordinates. The source is clearly extended beyond the nominal extension of the PSF (Fig. 1). A fit of a Gaussian folded with the PSF of the H.E.S.S. instruments gives an extension of  $0.18^\circ \pm 0.02^\circ$ .

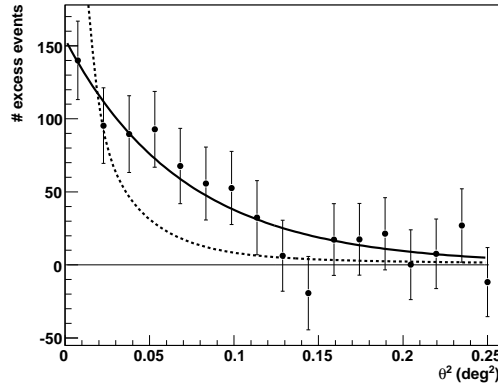


Figure 1: Number of excess events versus the squared angular distance from the best fit position of the excess. The dashed line shows the expectation for a point source derived from Monte Carlo data. The solid line is a fit of the PSF folded with a Gaussian ( $\sigma = 0.18^\circ \pm 0.02^\circ$ ).

The differential energy spectrum for photons inside the corresponding 85% containment radius of  $0.39^\circ$  is shown in Fig. 2. It can be described by a power law ( $dN/dE = \Phi_0 \cdot (E/1 \text{ TeV})^{-\Gamma}$ ) with a photon index of  $\Gamma = 2.53 \pm 0.16_{\text{stat}} \pm 0.1_{\text{syst}}$  and a normalization at 1 TeV of  $\Phi_0 = (4.50 \pm 0.56_{\text{stat}} \pm 0.90_{\text{syst}}) \times 10^{-12} \text{ TeV}^{-1} \text{ cm}^{-2} \text{ s}^{-1}$ . The integral flux for the whole excess above the energy threshold of 380 GeV is  $(1.3 \pm 0.3) \times 10^{-11} \text{ cm}^{-2} \text{ s}^{-1}$ . No significant flux variability could be detected in the data set. The fit of a constant function to the lightcurve binned in data segments of 28 minutes has a chance probability of 0.14. The results were checked with independent analyses and found to be in good agreement.

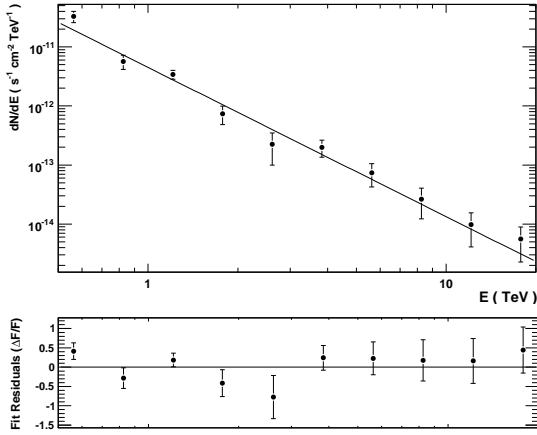


Figure 2: Differential energy spectrum and residuals to a single power-law fit of HESS J1023–575 from photons inside the 85% containment radius ( $0.39^\circ$ ) around the best fit position. The background is estimated with background regions of the same size and distance from the camera center as the signal region.

### HESS J1023–575 in the context of $\gamma$ -ray emission scenarios

The detection of VHE gamma-ray emission from the Westerlund 2 region [13] is proof for extreme high-energy particle acceleration associated with this young star forming region. With a projected angular size of submilliarcsecond scale, the WR 20a binary system, including its colliding wind zone, would appear as a point source for observations with the H.E.S.S. telescope array. Unless there are extreme differences in the spatial extent of the particle distributions producing radio, X-ray, and VHE gamma-ray emission, a *colliding stellar wind scenario* for the WR 20a binary faces the severe problem of accounting for the observed VHE source extension. At a nominal distance of 8.0 kpc, this source extension is equivalent to a diameter of 28 pc for the emission region, consistent in size with theoretical predictions of bubbles blown from massive stars into the ISM [14]. The spatial extension found for HESS J1023–575 contradicts emission scenarios where the bulk of the gamma-rays are produced close to the massive stars. Alternatively, the emis-

sion could arise from *collective effects of stellar winds* in the Westerlund 2 stellar cluster. Diffusive shock acceleration in cases where energetic particles experience multiple shocks can be considered for Westerlund 2. The stellar winds may provide a sufficiently dense target for high-energy particles, allowing the production of  $\pi^0$ -decay  $\gamma$ -rays via inelastic pp-interactions. Collective wind scenarios [15, 16] suggest that the spatial extent of the gamma-ray emission corresponds to the volume filled by the hot, shocked stellar winds, but HESS J1023–575 substantially supersedes the boundary of Westerlund 2. Supershells, molecular clouds, and inhomogeneities embedded in the dense hot medium may serve as the targets for gamma-ray production in Cosmic Ray interactions. Such environments have been studied in the non-linear theory of particle acceleration by large-scale MHD turbulence [17]. *Shocks and MHD turbulent motion inside a stellar bubble or superbubble* can efficiently transfer energy to cosmic rays if the particle acceleration time inside the hot bubble is much shorter than the bubble’s expansion time.

Finally, shock acceleration at the boundaries of the “blister” (Fig. 3 right) may enable particles to diffusively re-enter into the dense medium, thereby interacting in hadronic collisions and producing gamma-rays. A scenario as outlined in [18] for a Supernova-driven expansion of particles into a low density medium may be applicable to the expanding stellar winds into the ambient medium. If one accepts such a scenario here, it might give the first observational support of gamma-ray emission due to diffusive shock acceleration from supersonic winds in a wind-blown bubble around WR 20a, or the ensemble of hot and massive OB stars from a superbubble in Westerlund 2, breaking out beyond the edge of a molecular cloud. Accordingly, one has to consider that such acceleration sites will also contribute to the observed flux of cosmic rays in our Galaxy [19].

Further observations with the H.E.S.S. telescope array will help to discriminate among the alternatives in the interpretation of HESS J1023–575. However, the convincing association with a new type of astronomical object a massive HII region and its ionizing young stellar cluster profoundly distinguishes this new detection by the H.E.S.S. telescope array already from other source findings

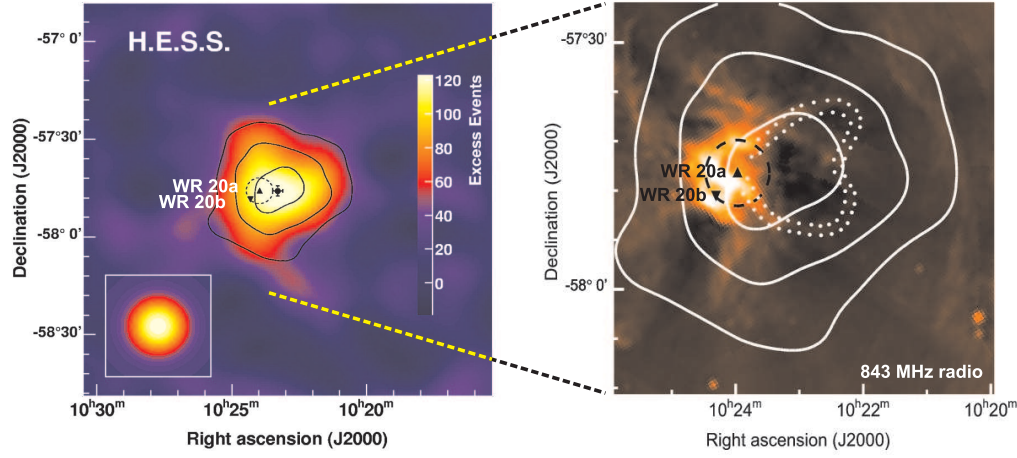


Figure 3: Left: H.E.S.S.  $\gamma$ -ray sky map of the Westerlund 2 region, smoothed to reduce the effect of statistical fluctuations. The inlay in the lower left corner shows how a point-like source would have been seen by H.E.S.S. WR 20a and WR 20b are marked as filled triangles, and the stellar cluster Westerlund 2 is represented by a dashed circle. Right: Significance contours of the  $\gamma$ -ray source HESS J1023–575 (corresponding 5, 7 and  $9\sigma$ ), overlaid on a MOST radio image. The wind-blown bubble around WR 20a, and the blister to the west of it can be seen as depressions in the radio continuum. The blister is indicated by white dots as in [4], and appears to be compatible in direction and location with HESS J1023–575.

made during earlier Galactic Plane Scan observations.

## Acknowledgements

The support of the Namibian authorities and of the University of Namibia in facilitating the construction and operation of H.E.S.S. is gratefully acknowledged, as is the support by the German Ministry for Education and Research (BMBF), the Max Planck Society, the French Ministry for Research, the CNRS-IN2P3 and the Astroparticle Interdisciplinary Programme of the CNRS, the U.K. Science and Technology Facilities Council (STFC), the IPNP of the Charles University, the Polish Ministry of Science and Higher Education, the South African Department of Science and Technology and National Research Foundation, and by the University of Namibia. We appreciate the excellent work of the technical support staff in Berlin, Durham, Hamburg, Heidelberg, Palaiseau, Paris, Saclay, and in Namibia in the construction and operation of the equipment.

## References

- [1] Whitney, B. A. et al. 2004, *ApJS* 154, 315
- [2] Churchwell, E., et al. 2004, *ApJS* 154, 322
- [3] Conti, P. S. & Crowther, P. A. 2004, *MNRAS* 255, 899
- [4] Whiteoak, J. B. Z., & Uchida, K. I. 1997, *A&A* 317, 563
- [5] Rauw, G. et al. 2007, *A&A* 463, 981
- [6] Rauw, G. et al. 2005, *A&A* 432, 985
- [7] Rauw, G. et al. 2004, *A&A* 420, L9
- [8] Bonanos, A. Z. et al. 2004, *ApJ* 611, L33
- [9] Belloni, T., & Mereghetti, S. 1994, *A&A* 286, 935
- [10] Bednarek, W. 2005, *MNRAS* 363, L46
- [11] Reimer, A., Pohl, M. K., & Reimer, O. 2006, *ApJ* 644, 1118
- [12] Dubus, G. 2006, *A&A* 451, 9
- [13] Aharonian, F. et al. (*H.E.S.S. Collaboration*) 2007, *A&A* 467, 1075
- [14] Castor, J., McCray, R., & Weaver, R. 1975, *ApJ* 200, L107
- [15] Klepach, E. G., Ptuskin, V. S., & Zirakashvili, V. N. 2000, *Aph* 13, 161
- [16] Domingo-Santamaria, E. & Torres, D. F. 2006, *A&A* 448, 613
- [17] Bykov, A. M. & Toptygin, I. N. 1987, *Ap&SS* Vol.138, No.2, 341
- [18] Völk, H. J. 1983, *Space Sci. Rev.* 36, 3
- [19] Cassé, M. & Paul, J. A. 1980, *ApJ*, 237, 236
- [20] Ascenso, J. et al. 2007, *A&A* 466, 137